GEOLOGICAL JOURNAL
Geol. J. **41**: 557–580 (2006)
Published online 22 September 2006 in Wiley InterScience
(www.interscience.wiley.com) DOI: 10.1002/gj.1058

The genesis of the carbonatized and silicified ultramafics known as listvenites: a case study from the Mihalıççık region (Eskişehir), NW Turkey

MEHMET AKBULUT[1]*, ÖZKAN PİŞKİN[1] and ALİ İHSAN KARAYİĞİT[2]

[1]*Dokuz Eylül Üniversitesi, Jeoloji Mühendisliği Bölümü, Buca, İzmir, Turkey*
[2]*Hacettepe Üniversitesi, Jeoloji Mühendisliği Bölümü, Beytepe, Ankara, Turkey*

The Mihalıççık region (Eskişehir) in NW Turkey includes an ophiolitic assemblage with a serpentinite-matrix mélange. The serpentinites of this mélange host silica-carbonate metasomatites which were previously named as listvenites. Our mineralogical and geochemical studies revealed that these alteration assemblages represent members of the listvenitic series, mainly the carbonate rocks, silica-carbonate rocks and birbirites, rather than true listvenites (*sensu stricto*). Tectonic activity and lithology are principal factors that control the formation of these assemblages. Carbonatization and silicification of the serpentinite host-rock is generated by CO_2, SiO_2-rich H_2O hydrothermal fluid which includes As, Ba, Sb and Sr. Low precious metal (Au, Ag) contents of the alteration assemblages indicate lack of these metals in the fluid. Primary assemblages of the alteration are carbonate rocks that are followed by silica-carbonate rocks and birbirites, respectively. Petrographic studies and chemical analyses suggested an alkaline and moderate to high temperature (350–400°C) fluid with low oxygen and sulphur fugacity for the carbonatization of the serpentinites. The low temperature phases observed in the subsequent silicification indicated that the fluid cooled during progressive alteration. The increasing Fe-oxide content and sulphur phases also suggested increasing oxygen and sulphur fugacity during this secondary process and silica-carbonate rock formation. The occurrence of birbirites is considered as a result of reactivation of tectonic features. These rocks are classified in two sub-groups; the Group 1 birbirites show analogous rare earth element (REE) trends with the serpentinite host-rock, and the Group 2 birbirites simulate the REE trends of the nearby tectonic granitoid slices. The unorthodox REE trend of Group 2 birbirites is interpreted to have resulted from a mobilization process triggered by the weathering solutions rather than being products of enrichment by the higher temperature hydrothermal activity.

Received 4 April 2005; revised version received 24 May 2006; accepted 21 June 2006

KEY WORDS ophiolite; listvenite; silica-carbonate alteration; Eskişehir-Mihalıççık; Turkey

1. INTRODUCTION

One of the important concerns of mineral research and exploration are the alteration products that are valuable indicators for exploration geologists. Hydrothermal/metasomatic alteration products, that is metasomatites, are naturally related to the mineralogy of the host rocks and the fluid nature. Infiltration of hydrothermal fluids in ultramafic terrains results in significant and a wide spectrum of metasomatites which are documented by several authors (e.g. Rose 1837, 1842; Murchison *et al.* 1845; Lodochnikov 1936; Borodayevskiy and Borodayevskiy

* Correspondence to: M. Akbulut, Dokuz Eylül Üniversitesi, Jeoloji Mühendisliği Bölümü, Buca, TR-35160 İzmir, Turkey.
E-mail: makbulut@deu.edu.tr

1947; Bok 1956; Ploshko 1963; Kashkai and Allakhverdiev 1965, 1971; Shcherban 1967; Shcherban and Borovikova 1969; Goncharenko 1970; Abovian 1978; Kuleshevich 1984; Ivan *et al.* 1985; Buisson and Leblanc 1985, 1986, 1987; Aydal 1989; Nixon 1990; Ash and Arksey 1990a,b; Madu *et al.* 1990; Spiridonov 1991; Auclair *et al.* 1993; Halls and Zhao 1995; Uçurum 1996, 2000). Listvenites (quartz-carbonate-chromium mica association), quartz-carbonate rocks (silica-carbonate association), carbonate-rich rocks, serpentine-talc-(chlorite)-carbonate rocks, talc-carbonate rocks and talc-silica-carbonate rocks are the examples of the metasomatites. Listvenites, spatially associated with low temperature Ag, Hg, As, Co and Ni mineralizations and deposits worldwide are the most important of these metasomatites (e.g. Kashkai and Allakhverdiev 1965; Russia: Gorchakov and Lishnevskiy 1982; Goncharenko 1984; Buisson and Leblanc 1986; Korobeynikov and Goncharenko 1986; Morocco: Leblanc and Lbouabi 1988; Leblanc and Fischer 1990; Canada: Auclair *et al.* 1993; USA: Sherlock and Logan 1995; Ireland: Halls and Zhao 1995; Turkey: Uçurum 1996, 2000; Egypt: Botros 2002).

The term listvenite was first introduced by the Russian geologist Rose (1837, 1842) to define the silica-carbonate metasomatites enclosing gold-bearing quartz lodes in Ural goldfields. Rose (1842) defines the listvenite as an assemblage of carbonate (magnesite/ankerite), quartz and fuchsite (Cr-muscovite) with disseminated pyrite and accessory minerals (Halls and Zhao 1995). He indicates that the fresh hand specimens of the rock present a granular green and white flecked appearance due to the mixture of white coloured carbonates and green coloured fuchsite, although sometimes gaining a brown appearance caused by weathering of ankerite/magnesite to limonite. Listvenites form by intermediate-low temperature hydrothermal/metasomatic alteration of mafic-ultramafic rocks (especially serpentinites) and are commonly located within or near major fault and shear zones (Halls and Zhao 1995). With the influx of K-bearing hydrothermal fluids in the tectonic fractures, primary ferromagnesian silicates of host rocks are replaced by the Mg-Fe (-Ca) carbonates. Silica is released to form quartz; and with introduction of potassium via fluid, fuchsite forms.

The term listvenite was used by several researchers to describe various carbonatized and silicified alteration assemblages with different phyllosilicate minerals in mafic-ultramafic terranes. Detailed history of these studies and the nomenclature was recently compiled by Halls and Zhao (1995). In summary, the listvenites bear Cr-mica and represent the beresitic facies, whereas the listvenite-like metasomatites include Cr-clay minerals and represent the argillic facies of metasomatites in ultramafic terranes (Spiridonov 1991; Halls and Zhao 1995).

Numerous listvenites and listvenite-like metasomatites have been studied along the Alpine belts (e.g. Rose 1842; Spiridonov 1991; Auclair *et al.* 1993; Halls and Zhao 1995). In Turkey, several mineralized and non-mineralized listvenitic occurrences are scattered within the serpentinized ultramafic portions of the ophiolites along the İzmir-Ankara-Erzincan Suture (İAES), a part of the Alpine belt (e.g. Lisenbee 1971; Şentürk and Karaköse 1981; Aydal 1989; Erler and Larson 1990; Genç *et al.* 1990; Tüysüz and Erler 1993; Boztuğ *et al.* 1994; Koç and Kadıoğlu 1996; Uçurum 1996, 2000; Gözler *et al.* 1997; Uçurum and Larson 1999).

One of the mineralized listvenitic occurrences along IAES is located in Kaymaz (Sivrihisar, NW Turkey). These occurrences are enriched in precious metals at ore grade (e.g. 3 g Au/t) (Erler and Larson 1990; Larson and Erler 1992; Uçurum 2000). Silver concentrations, ranging between 0.0004 g/t and 10.2 g/t, are reported from Yunus Emre which is located NE of Kaymaz (Koç and Kadıoğlu 1996; Reçber *et al.* 1997; Uçurum 2000).

The present study deals with the alteration products within the serpentinite-matrix mélange in Mihalıççık (Eskişehir) region which were previously named as 'listvenites' by Gözler *et al.* (1997). The present study was carried out during the 2002–2003 period of Sivrihisar Polymetal Prospect, held by the General Directorate of Mineral Research and Exploration (MTA) of Turkey. The study area is selected due to the proximity of Mihalıççık region metasomatites to Kaymaz and Yunus Emre mineralized listvenites and the promising stream sediment and rock chip sampling data of MTA. The aims of this study are to present the geological, mineralogical and geochemical characteristics of the alteration assemblages in the Mihalıççık region, and to contribute to the genetic problem of rocks of listvenitic series. Mineralization in the alteration products is also discussed.

DOI: 10.1002/gj

2. GEOLOGICAL SETTING

2.1. Regional geology

Western Turkey comprises several continental fragments amalgamated by the Early Tertiary continent–continent collision, following the obliteration of Tethyan oceanic lithospheres (Şengör and Yılmaz 1981; Okay 1989). Some of these fragments, namely, the Sakarya Terrane and Tavşanlı and Afyon zones of the Anatolide-Tauride Block, are separated by the İAES in northwestern Turkey. The İAES is a boundary zone that is regarded as a remnant of oceanic basins between two converging continents, Gondwanaland and Eurasia. The northern segment of the İAES represents the northern branch of the Neotethyan Ocean which was entirely consumed along a north-dipping intra-oceanic subduction zone during early Late Cretaceous time (e.g. Göncüoğlu and Türeli 1993; Yalınız *et al.* 1996; Floyd *et al.* 1998; Göncüoğlu *et al.* 2000). Okay *et al.* (2001) indicate that during the Campanian, the Anatolide-Tauride Block had subducted 60 km under the Sakarya continent, resulting in blueschist metamorphism under conditions of 20 kbar pressure and 440°C temperature. In the north of the Anatolide-Tauride Block, ultramafic rocks are found either directly on the blueschist facies rocks or on a mélange slab (accretionary mélange) bordering the blueschists (Okay 1984; Okay *et al.* 2001). The age of peak blueschist metamorphism is constrained to 80 ± 5 Ma by Rb-Sr and Ar-Ar isotopic data (Campanian: Okay and Kelley 1994; Sherlock *et al.* 1999; Okay *et al.* 2001). Several granodiorite plutons with Early to Middle Eocene Ar-Ar isotopic ages (53–48 Ma) intrude the blueschists, accretionary complex and ophiolites (Harris *et al.* 1994; Sherlock *et al.* 1999; Okay *et al.* 2001). The study area is located in this blueschist belt, south of the İAES (Figure 1).

2.2. Local geology

The basement rocks in the study area, namely the Mihalıççık metamorphics (Figure 2) including graphite schists with sericite, muscovite and graphite, are characterized by micro- and small-scale folds and joints. Chlorite-actinolite assemblage of typical greenschist facies, with amphibole microlithes, Mg-chlorites and coarse pyroxene porphyroclasts, accompany these rocks. The presence of glaucophane schists composed of lawsonite, albite, epidote and glaucophane indicates a transition from greenschist to blueschist facies. The metamorphic basement also includes pink coloured quartzite layers, which contain coarse- to fine-grained quartz and accessory mica.

A serpentinite-matrix mélange rests on the metamorphic rocks with a thrust and is unconformably overlain by the sediments of the Porsuk Formation (Figures 2 and 3). This association contains intensely deformed serpentinites, cherts, mudstones and blocks of recrystallized limestones. The silica-carbonate metasomatites are hosted by the serpentinites of the mélange. These alteration-related reaction zones present a noticeable rocky morphology and mark the former fracture zones. However, the exposure of metasomatites along these former tectonic features makes it impossible to observe any kind of field evidence on type of fractures. Several large and small dyke or pod-like alteration bodies, which are locally overlain by Neogene cover, are scattered to the north and southeast of the study area. In the southern part of the study area, the metasomatites are exposed within the serpentinites with a strike of N70°W and dip of 75°SW. The outcrop is about 1750 m in length and is cross-cut by E–W-trending faults (Akbulut 2003) that cause sharp turns in the strike of the outcrop (Figure 2). Similar structures can be observed in the northeast of the study area. Field observations indicate that lithology and tectonics control the formation of the studied metasomatites. The superposition of Neogene cover on the metasomatites suggests that formation of the fractures had taken place between the Maastrichtian and Middle Miocene, before the deposition of the Porsuk Formation.

The granitoids in the study area are intensely altered and weathered with respect to other Tertiary granites located in the south, outside the study area (Figure 1). They are also mylonitized and foliated with characteristic cataclastic texture (e.g. undulatory extinction of quartz crystals in thin sections) that indicate dynamo-metamorphic history. No sign of thermal metamorphism is observed along the contacts of the granitoids and within the serpentinite-matrix mélange. Moreover, a slice of serpentinite is wedged within the granitoid body in the east of the area (Figures 2 and 3). All of these observations suggest that the granitoids are fragments of a

DOI: 10.1002/gj

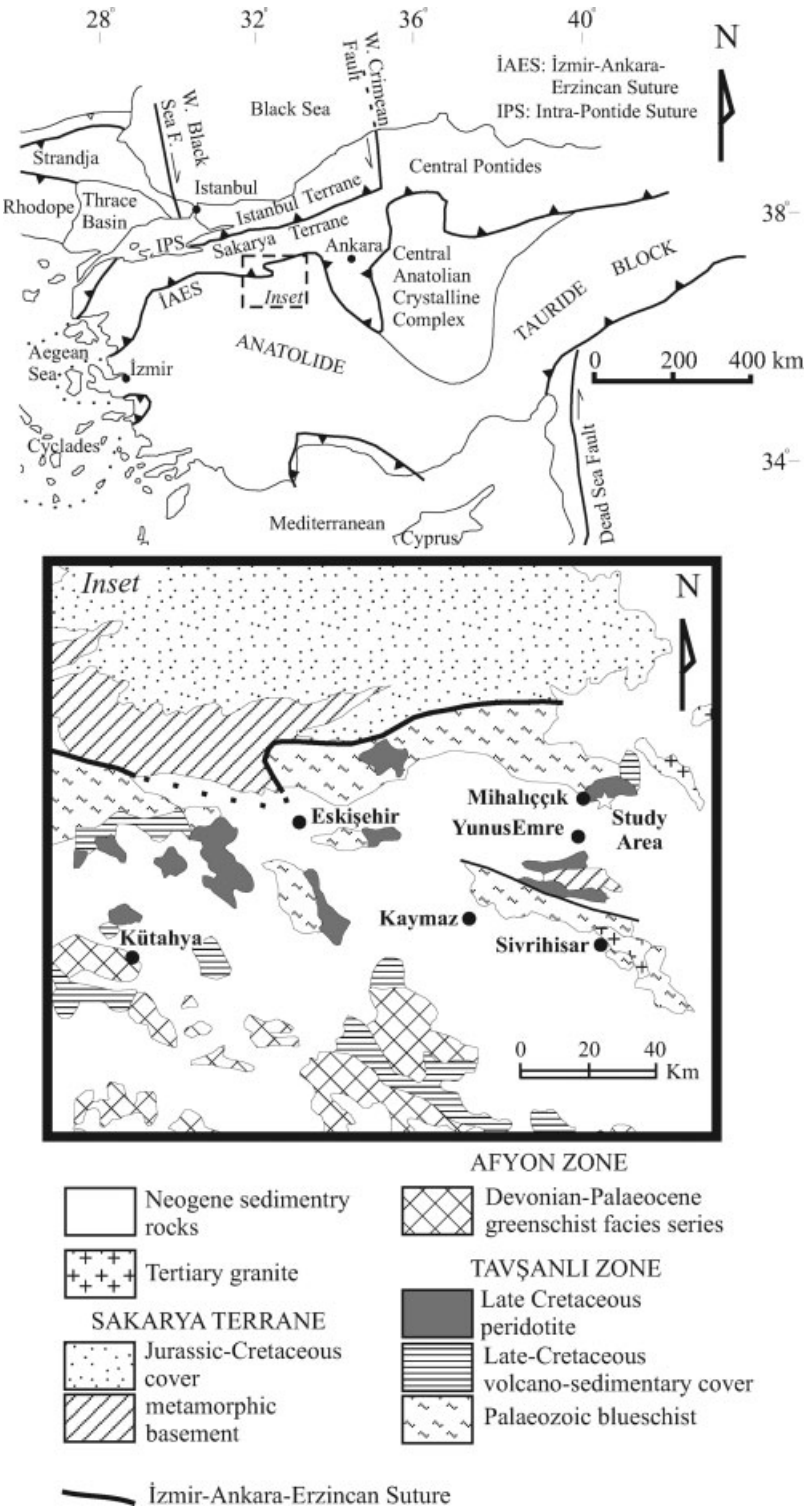

Figure 1. Regional geology and location of the study area (tectonic units map of Turkey simplified from Okay and Göncüoğlu 2004, inset map modified from Okay *et al.* (1998)).

DOI: 10.1002/gj

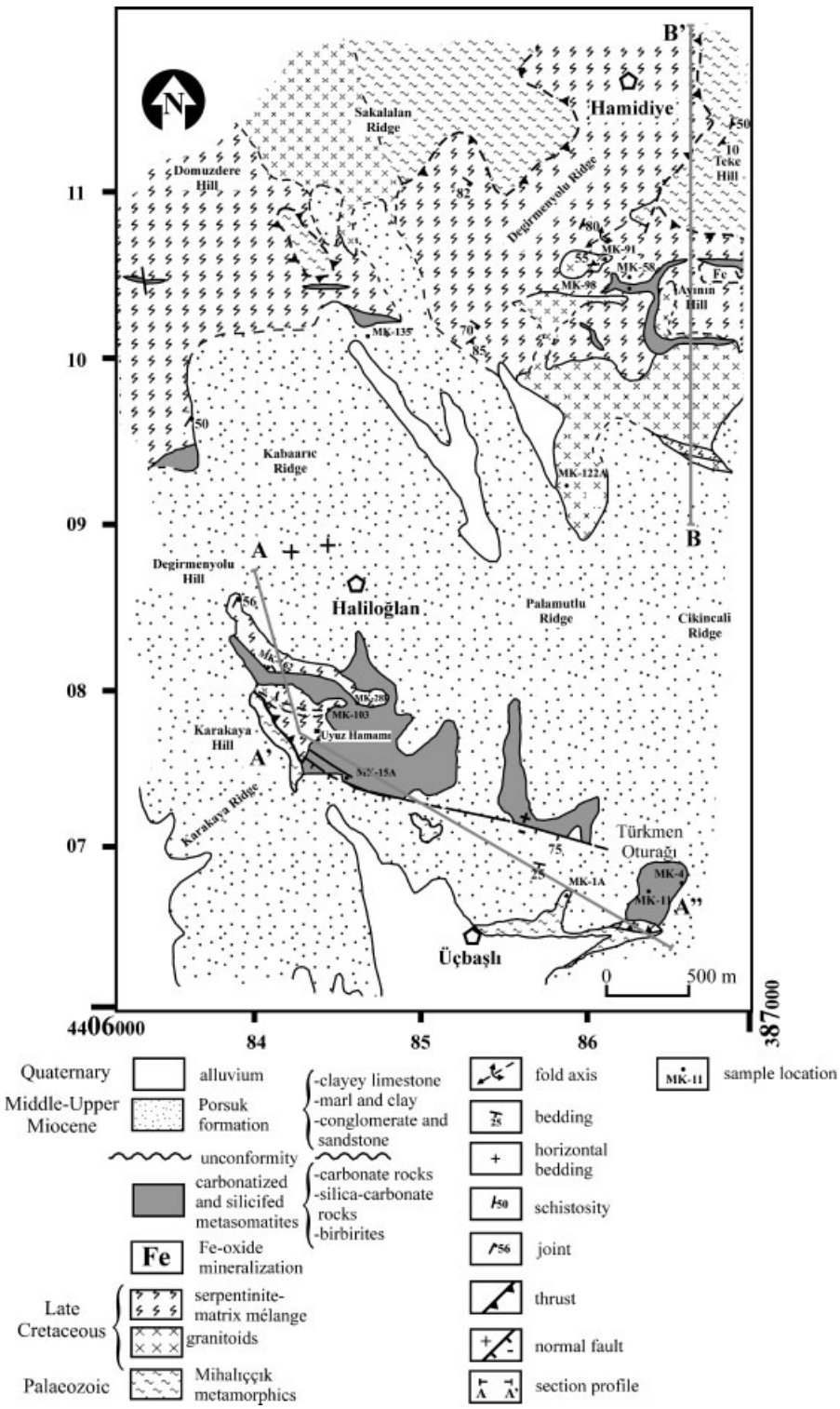

Figure 2. Geological map of the study area (modified from Akbulut 2003).

DOI: 10.1002/gj

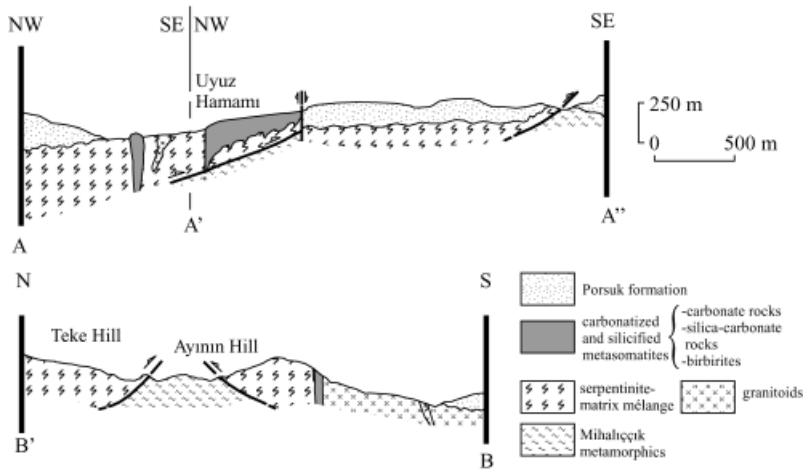

Figure 3. Geological cross-sections of the study area. See Figure 2 for locations and profiles.

former intrusion; they are sliced and tectonically included into the obducting serpentinite-matrix mélange. Our contention is consistent with the arguments of Delaloye and Bingöl (2000), who reported such tectonic contacts between post-Maastrichtian–Eocene formations and granitoid bodies in the area between east of Eskişehir and Bilecik, south of the İAES.

3. PETROGRAPHY OF THE HOST-ROCK AND THE METASOMATITES

Petrographic studies of the samples compiled from the study area were carried out on both the host rock and the metasomatites. Thin and polished sections of the hand specimens were examined at Dokuz Eylül University, İzmir (Turkey).

3.1. The Host-rock

Serpentinites form the host-rocks to alteration under consideration. They are composed mainly of chrysotile, antigorite, lizardite, bastite, pyroxene and olivine. Disseminated chromite, chromium-spinel, magnetite, pyrite (pyrite I), limonite, haematite, goethite, hypidiomorphic pyrite (pyrite II), very fine-grained heazlewoodite (?) and minor gold (electrum) accompany the rock-forming minerals. These rocks are characterized by typical serpentinite mesh texture.

3.2. The Metasomatites

Microscopic studies on the silica-carbonate dykes and pods reveals three basic types of metasomatites: (i) carbonate rocks, (ii) silica-carbonate rocks and (iii) birbirites.

(i) *Carbonate rocks*: These rocks are greenish-yellow and yellow coloured in hand specimens. They are composed dominantly of fine- to medium-grained rhombohedral dolomites with accessory amount of goethite and limonite in thin sections. They do not show any sign of primary rock texture (Figure 4a).

(ii) *Silica-carbonate rocks*: These are yellowish-brown and brown coloured, and consist mainly of silica and dolomite with rare opaque minerals (chromite, magnetite, pyrite, marcasite, haematite and goethite). These rocks show heterogeneity in modal composition. The main carbonate phase in the rock is dolomite. The rocks are primarily carbonatized along fractures and pores. Silica is a secondary phase observed as radial pore infill and microcrystalline quartz veins which cross-cut the primary carbonate veins and pores (Figure 4b,c). The calcites in secondary silica veins are precipitates of a later stage (Figure 4d). Carbonates, silica and bowlingite

DOI: 10.1002/gj

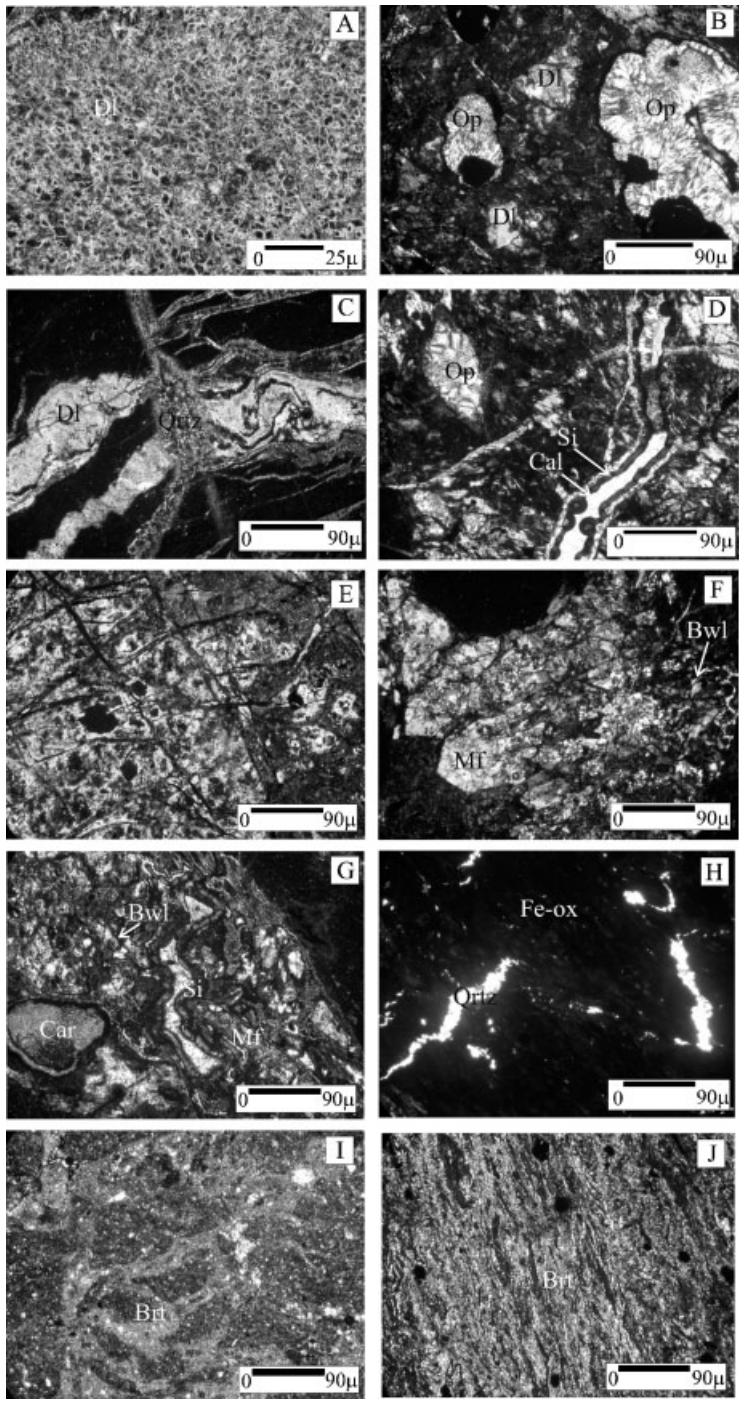

Figure 4. Photomicrographs of the silica-carbonate metasomatites (crossed polars); Dl, dolomite; Op, opal; Qrtz, quartz; Cal, calcite; Bwl, bowlingite; Mf, carbonatized mafic mineral; Si, silica; Fe-ox, iron oxide; Brt, birbirite Car, carbonate. (a) rhombohedral dolomites in carbonate rocks; (b) and (c) silica overprint in primarily carbonatized rocks as radial pore infills and veins; (d) second stage of carbonatization in form of calcite veins; (e) stockwork-like texture in silica-carbonate rocks; (f) and (g) relict minerals of the original lithology (bowlingite and carbonatized mafic minerals) surrounded by colloform and radial silica; (h) silica- and iron-rich sample (MK-26); (i) ghost texture of breccia in birbirite; (j) mylonitization in birbirite.

DOI: 10.1002/gj

create a stockwork-like texture in some specimens (Figure 4e). Carbonatized mafic minerals and bowlingite are surrounded by colloform and radial silica (Figure 4f,g). Also, some portions of this type show a silica-rich and carbonate-free mineralogy (sample *MK 26*). These include only silica as fine-grained quartz crystals and Fe-oxides (Figure 4h). Marcasite in the silica-carbonate rocks is partly transformed into colloidal goethite. Pyrite I is totally transformed into haematite and goethite but its euhedral structure is preserved.

(iii) *Birbirites*: The brown coloured compact quartzites are named as birbirites (Tomkeieff 1983); they are free of carbonates and are composed of only microcrystalline quartz, coarse quartz veinlets, radial opal and opaque minerals. The opaques are magnetites formed from chromite grains due to alteration, arsenopyrite, glaucodot, bravoite (NiS-nickeliferous pyrite), gersdorffite, skutterudite (?), marcasite, haematite and goethite. This silicified rock shows a brecciated and mylonitized texture and does not contain any carbonate minerals. Ghost texture of breccia is hardly observed due to intense silicification (Figure 4i). Mylonitization related to tectonic activity is apparent (Figure 4j) in some thin sections. Fractures in the rock contain colloform quartz and Fe-oxides and euhedral pyrite crystals. XRD data support this quartz dominant mineralogy with minor kaolinite (?).

The mineralogy of the silica-carbonate metasomatites in the study area is consistent with the descriptions of alteration assemblages studied in Turkey (Araç Massif (Kastamonu): Aydal 1989; Kağızman Region (Kars): Tüysüz and Erler 1993; Alacahan Region (SE Sivas): Boztuğ *et al.* 1994; Karacakaya (Eskişehir): Koç and Kadıoğlu 1996; Cürek-Divriği (Sivas) and Güvenç-Karakuz-Hekimhan (Malatya): Uçurum 1996, 2000). Because, Cr-mica (fuchsite) is absent in the metasomatites of the study area, the alteration assemblages of Mihalıççık region are not proper listvenites but members of the listvenitic series with respect to the description of Halls and Zhao (1995).

The temporal phase relations indicate a primary stage of carbonatization that took place before the subsequent silicification. The spatial distribution of the alteration products are not apparent in all of the outcrops; however, in Türkmen Oturağı district (Figure 2), thin section studies showed that the carbonate assemblages change into silica-carbonate rocks in the altered body northeastwards. The birbirites in Uyuz Hamamı and west of Ayının Hill are located at the intersections of cross-cutting structures (Figure 2). This temporal and spatial transition seems to be in good agreement with the descriptions of the alteration products of New Almaden deposit (USA: Bailey and Everhart 1964), the Zod deposit (Armenia: Spiridonov 1991), the Eastern Metals deposit (Canada: Auclair *et al.* 1993) and the listvenites of Kağızman region (Turkey: Tüysüz and Erler 1993).

4. GEOCHEMISTRY

4.1. Analytical methods

Whole-rock chemical analyses of powdered rock samples from the study area were carried out at ACME Analytical Laboratories (Canada) for major oxides and trace elements by Inductively Coupled Plasma-Emission Spectrometry (ICP-ES) and Inductively Coupled Plasma-Mass Spectrometry (ICP-MS), respectively. Detection limits for major oxides by ICP-ES, and trace elements by ICP-MS are between 0.001 and 0.004%, and 0.01 and 0.5 ppm, respectively. Results of some major oxide samples were obtained by a Philips PW-1480 fully automatic X-Ray Fluorescence Spectrometer (XRF) fitted with a 3.0 kW, 100 kV Rh-anode, at Hacettepe University (Ankara-Turkey). Detection limits for major oxides by XRF are between 0.0007 and 0.027%. Minerals of some samples were also identified by X-ray powder diffraction (XRD) analysis using a CuKa tube ($2^\circ\,\mathrm{min}^{-1}$ scan speed, 0.02° step size and $2–40^\circ$ 2θ) at Hacettepe University. The specific gravities of the samples used for calculation of major-oxide gains and losses during metasomatism were determined at Dokuz Eylül University by picnometer tests.

4.2. Major oxides

Major oxide compositions of specimens from the host-rock and the metasomatites are given in Table 1. It is apparent that SiO_2, Al_2O_3, Fe_2O_3, MgO and CaO are the most variable major oxides that are mobilized during the

DOI: 10.1002/gj

Table 1. Major oxide concentrations of the metasomatites and the serpentinites in the study area

Samples	MK 8	MK 11	MK 29	MK 24	MK 26	MK 7	MK-6	MK 164	MK 4	MK 15A	MK 104A	MK 56-I	HMK 3	MK 98	MK 103	MK 58	HMK 18
Rock type	CR	CR	CR	CR	SIIR	SCR	SCR	SCR	SCR	SCR	BRT	BRT	BRT	BRT	BRT	SER	SER
SiO_2	2.52	4.58	4.45	6.83	47.15	59.44	40.00	58.82	52.49	68.84	81.24	89.74	81.81	84.35	88.13	38.19	37.13
Al_2O_3	0.42	1.25	1.06	1.40	0.46	0.21	0.19	0.08	0.40	0.59	0.35	2.48	8.85	7.89	0.41	0.56	1.64
Fe_2O_3	1.00	3.11	4.12	1.82	43.90	7.20	5.88	5.48	6.23	6.15	13.38	5.02	2.11	1.10	2.78	10.39	8.78
MgO	20.33	19.09	17.90	20.88	0.21	6.87	11.91	7.46	7.70	8.94	0.32	0.18	0.13	0.10	2.36	35.41	37.41
CaO	29.93	28.3	28.75	24.81	0.09	9.15	15.88	10.47	11.10	0.92	0.08	0.06	0.07	0.18	0.12	0.63	0.27
Na_2O	0.02	0.04	0.01	0.01	0.01	0.01	0.01	0.02	0.04	0.03	0.01	0.01	0.02	0.02	0.02	0.01	0.01
K_2O	0.00	0.03	0.03	0.04	0.04	0.04	0.04	0.04	0.02	0.02	0.04	0.43	0.39	0.33	0.02	0.04	0.02
TiO_2	0.01	0.03	0.03	0.05	0.01	0.01	0.01	0.01	0.01	0.01	0.01	0.10	0.34	0.34	0.01	0.01	0.02
P_2O_5	0.02	0.02	0.02	0.01	0.17	0.03	0.03	0.04	0.03	0.01	0.06	0.06	0.13	0.06	0.01	0.03	0.10
MnO	0.02	0.02	0.20	0.02	0.07	0.10	0.09	0.08	0.08	0.04	0.04	0.01	0.01	0.01	0.01	0.07	0.09
Cr_2O_3	0.09	0.16	0.09	0.13	0.56	0.65	0.41	0.23	0.978	0.835	1.049	0.004	0.38	0.007	0.336	0.50	0.371
LOI	0.21	0.7	0.91	43.9	6.60	16.1	25.5	17.10	20.80	13.40	3.10	1.70	6.00	5.60	5.60	13.8	14.00
TOT/S	n.a.	n.a.	n.a.	0.01	0.01	0.01	0.01	0.01	0.01	0.20	0.07	0.03	1.11	0.73	0.91	0.01	0.01
SUM	99.79	99.81	100.07	99.87	99.82	99.85	99.99	99.88	99.94	99.97	99.79	99.82	99.89	99.98	99.91	99.89	100

CR, carbonate rock; SIIR, silica- and iron-rich rock; SCR, silica-carbonate rock; BRT, birbirite; SER, serpentinite. n.a.; not analyzed.
All of the major oxides are in wt%.

DOI: 10.1002/gj

alteration process. Especially, the silica variation is pronounced. For instance, silica-carbonate rocks have higher concentrations of SiO_2 (average 55.92 wt%) than the serpentinites (average 37.66 wt%), while the silica concentration in birbirites exceeds 80 wt%. The carbonate rocks, in contrast, have lower amounts of silica (average 4.60 wt%) and higher amounts of MgO and CaO (average 19.55 and 27.95wt%, respectively). Fe_2O_3 values are generally lowered with respect to the average serpentinite (average 9.59 wt%) in all types of metasomatites (average 2.51; 6.19 and 4.88 wt % in carbonate rocks, silica-carbonate rocks and birbirites, respectively) except one sample which is rich in Fe_2O_3 and SiO_2 (*MK 26*, Table 1). Except for this sample (see X on Figure 5a), all samples plotted along the SiO_2-MgO pseudo-binary on SiO_2-Fe_2O_3-CaO+MgO ternary diagram.

Generation of different mineralogical assemblages during progressive alteration results in changes in contents of major oxides and trace elements. Several methods are suggested and applied to observe this elemental mobility

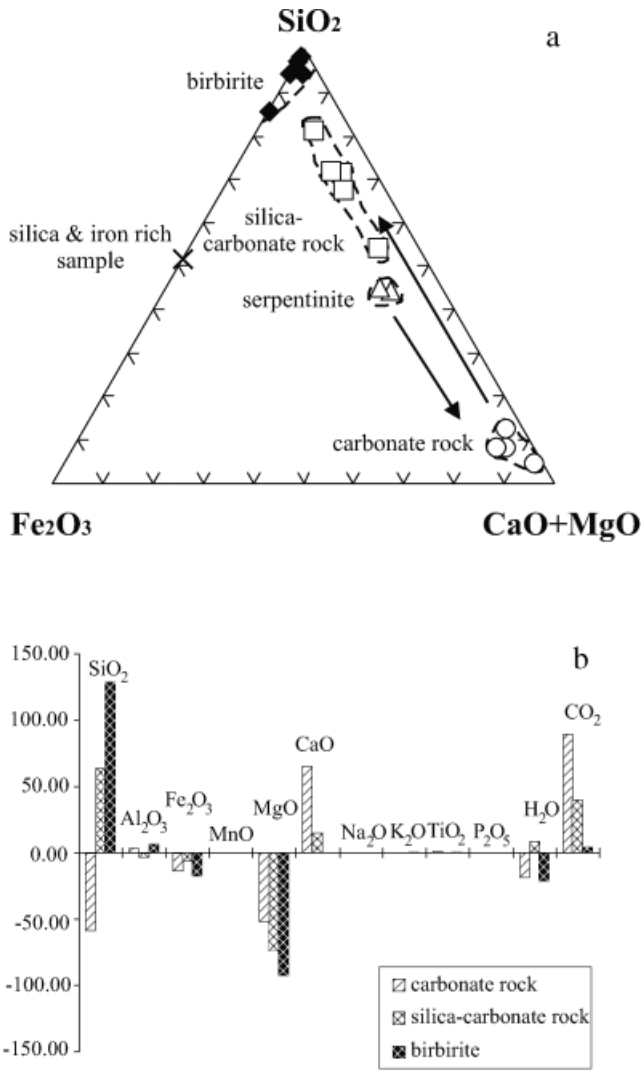

Figure 5. **(a)** Distribution of the silica-carbonate metasomatites and the serpentinites on the SiO_2-Fe_2O_3-CaO+MgO ternary diagram. (△) serpentinite; (○) carbonate rocks; (□) silica-carbonate rocks; (◆) birbirites; (×) silica- and iron- rich sample (MK-26). **(b)** Major oxides gains and losses during progressive alteration.

DOI: 10.1002/gj

during alteration (e.g. Gresens 1967; Grant 1986; Genç *et al.* 1990; MacLean 1990; Pirajno 1992; Abu El-Enen *et al.* 2004). The mass-balance calculation equation suggested by Gresens (1967) and rearranged by Grant (1986) contains two dependent variables (mass-X_n and volume f_v). MacLean and Kranidiotis (1987) have suggested procedures to fix the mass variable for many altered rock systems. However, the method was designed essentially for single precursor rocks and ophiolites and basalt-dominated stratigraphy should not be treated as single precursor systems without proper testing (MacLean 1990). Thus, changes in major oxide concentrations of the rocks in this study are computed using the method suggested by Genç *et al*. (1990), who also applied this method on the silica-carbonate-talc alteration products and serpentinites of Narman-Karadağ ophiolitic complex (Erzurum-Turkey). In this method, gains and losses in the metasomatites during alteration are calculated by multiplying the specific gravity of the rock with the analytical values of the major oxides and obtaining their differences. The negative (−) results reflect the losses whereas positive (+) ones mark the gains. Constant-volume assumption is unrealistic in metasomatism. However, large volume changes are also unlikely due to rock mechanical reasons (cf. Abu El-Enen *et al.* 2004). To consider the changes in volume, the specific gravities of the samples from the study area were determined by picnometer tests. The results, computed by using major oxides averages of selected representative samples of the study area, are given in Figure 5b. Carbonate rocks are depleted in SiO_2, Fe_2O_3, MgO, H_2O and enriched in Al_2O_3, CaO, TiO_2, CO_2 with respect to the serpentinite. The silica-carbonate rocks are enriched in SiO_2, CaO, H_2O and CO_2, and depleted in Fe_2O_3, MgO and Al_2O_3. The calculations for birbirites show that excessive amount of SiO_2 has been introduced into the rock together with enrichment in Al_2O_3 and CO_2. There is also an evident loss of MgO and depletion in Fe_2O_3 and H_2O in these rocks.

4.3. Trace and rare earth elements (REE)

Representative trace element contents of the rocks are given in Tables 2 and 3. Average REE and trace element concentrations of the metasomatites normalized to chondrite and MORB values are plotted in Figure 6. La values in one of the three carbonate rock samples is extreme (71.50 ppm), whereas the other two carbonate rock samples show La values below 0.50 ppm. A similar anomaly can be seen in serpentinite samples; one of the two samples is high in La (19.60 ppm), while in the other the La content is below 0.05 ppm. These diverse La values of the samples are interpreted as analytical errors. Thus, instead of La, Ce is plotted in the diagrams and taken into consideration in LREE evaluation. Generally, REE concentrations of the alteration assemblages show complex zig-zag patterns, except for the average of three samples of birbirites (Figure 6a). The only SiO_2 and Fe_2O_3 rich altered sample (*MK-26*) plotted on the diagram shows a clean convex upwards pattern from Ce to Lu. The REE concentrations of the carbonate rock samples (open circles) are scattered around ∼1 log unit above and 6 log units below the chondritic values. The silica-carbonate rocks (open squares) also follow similar trends like the carbonate rocks with lower contents in HREE. Even though there are significant differences in the MREE contents, a rough affinity can be determined between the REE trends of the serpentinites (open triangles), carbonate rocks, silica-carbonate rocks and two of the birbirite samples (closed squares). The REE patterns of the remaining birbirites (open diamonds), on the contrary, show a significantly enhanced REE abundance on the chondrite-normalized plot with a gentle negative slope from LREE to HREE. Here, it must be noted that these birbirites (open diamonds) are sampled from the outcrops that are juxtaposed to the granitoid slices. Due to the clearly different REE patterns, the birbirites are subgrouped as: (i) Group 1, which has the similar REE trends with the other fresh and altered rocks, and (ii) Group 2, which shows a general REE enrichment trend.

In order to obtain a measure of relative change during alteration, REE contents of the alteration assemblages are normalized to average REE values of the host-rock serpentinites (Figure 6b). A general analogy between the REE trends of all the alteration products is remarkable in this plot. Even the Group 2 birbirites separated from the others by their REE abundances show the same complex and sinusoidal patterns like the rest of the alteration products while protecting their negative trend from LREE to HREE.

The REE are considered as relatively immobile elements during low grade metasomatism and hydrothermal alteration (Rollinson 1993). Hence, the analogous REE patterns may indicate the genetic relation of the alteration products, particularly the common primitive lithology. However, the significantly enhanced REE contents of the

DOI: 10.1002/gj

Table 2. Trace and rare earth element concentrations of the metasomatites, serpentinites and the granitoids in the study area

Samples	MK 11	MK 24	MK 29	MK 26	MK 7	MK 6	MK 164	MK 4	MK 15A	MK 104A	MK 56-I	HMK 3	MK 98	MK 103	MK 58	HMK 18
Rock type	CR	CR	CR	SIIR	SCR	SCR	SCR	SCR	SCR	BRT	BRT	BRT	BRT	BRT	SER	SER
Sc	n.a.	20.00	n.a.	25.20	94.80	3.00	5.00	6.00	3.00	11.00	12.00	10.00	5.00	1.00	9.00	12.00
Ba	59.70	66.00	5.40	25.20	94.80	49.20	75.80	28.00	374.00	205.60	383.50	47.70	43.00	9.00	19.50	8.00
Co	15.00	11.80	64.20	389.10	110.70	86.80	66.40	52.20	84.90	104.00	109.90	38.40	3.30	58.00	110.10	106.00
Hf	<0.50	<0.50	<0.50	<0.50	<0.50	<0.50	<0.50	<0.50	<0.50	<0.50	<0.50	1.90	1.60	<0.50	<0.50	<0.50
Nb	<0.50	<0.50	<0.50	<0.50	<0.50	<0.50	<0.50	<0.50	<0.50	<0.50	2.30	5.00	4.40	0.50	<0.50	<0.50
Rb	1.10	3.90	0.80	<0.50	3.00	2.20	3.30	<0.50	2.30	1.50	18.80	8.90	10.10	1.60	2.00	<0.50
Sr	211.30	621.60	57.10	9.30	117.10	139.20	149.60	95.20	25.80	8.80	154.70	176.50	176.00	3.60	6.90	3.50
Ta	<0.10	<0.10	<0.10	<0.10	<0.10	<0.10	<0.10	0.10	<0.10	<0.10	0.30	0.30	0.20	<0.10	<0.10	<0.10
Th	<0.10	<0.10	<0.10	<0.10	<0.10	<0.10	0.10	0.10	<0.10	<0.10	3.20	3.30	2.50	<0.10	<0.10	<0.10
V	80.00	79.00	57.00	202.00	54.00	48.00	37.00	59.00	42.00	158.00	30.00	58.00	51.00	20.00	38.00	69.00
Zr	2.50	1.30	0.80	3.30	1.70	3.90	4.50	5.20	0.70	1.30	21.40	61.90	62.00	1.20	1.20	<0.50
Y	3.40	3.00	1.30	4.80	0.60	0.70	0.70	1.10	0.20	2.30	17.40	16.00	15.00	1.20	0.30	0.50
Cr	1061	910.05	608.98	3832	4461	2792	1588	6706	5748	7178	27.37	260.02	68.43	2327	3808	2530
Mo	0.20	<0.10	0.10	14.90	0.80	0.60	0.60	0.70	0.70	7.50	1.80	0.40	0.30	0.30	0.20	0.10
Cu	75.20	23.90	13.20	56.70	6.30	5.70	8.30	13.60	13.20	24.00	38.60	28.30	14.80	6.60	1.10	54.60
Pb	1.90	0.10	0.10	0.50	1.40	1.00	1.50	3.80	2.10	0.30	10.90	5.30	10.50	2.90	0.20	3.50
Zn	7.00	4.00	4.00	41.00	13.00	12.00	13.00	23.00	17.00	21.00	101.00	3.00	11.00	24.00	19.00	16.00
Ni	414.40	110.80	369.10	3166	586.20	599.90	619.60	655.00	957.00	1093	280.30	21.40	15.30	881.00	2243	2112
As	141.60	13.40	3.50	760.70	183.90	276.60	177.00	209.00	366.00	763.20	118.30	39.10	15.20	1355	0.60	1.20
Sb	2.80	<0.10	0.30	5.40	1.20	0.30	1.20	2.10	0.70	1.90	0.40	0.10	0.10	0.20	<0.10	<0.10
Ag	0.10	0.30	0.30	0.50	0.10	0.10	0.10	<0.10	<0.10	0.30	0.10	0.30	<0.10	<0.10	0.10	<0.10
Au*	3.60	27.90	5.00	24.20	78.60	23.20	14.10	25.00	33.70	44.10	25.20	45.90	49.10	157.00	15.90	1.50
Hg	0.01	<0.01	0.02	<0.01	<0.01	<0.01	<0.01	0.01	0.16	<0.01	0.04	0.17	0.07	0.02	0.01	0.01
Tl	0.10	<0.10	<0.10	<0.10	<0.10	<0.10	0.10	0.10	0.10	<0.10	0.20	0.20	0.10	<0.10	<0.10	<0.10

CR, carbonate rock; SIIR, silica- and iron-rich rock, SCR, silica-carbonate rock; BRT, birbirite; SER, serpentinite; n.a.; not analyzed.
*All of the trace elements except the Au are in ppm. Au values are in ppb.

DOI: 10.1002/gj

Table 3. Trace and rare earth element concentrations of the metasomatites, serpentinites and the granitoids in the study area (continued)

Samples	MK 11	MK 24	MK 29	MK 26	MK 7	MK 6	MK 164	MK 4	MK 15A	MK 104A	MK 103
Rock type	CR	CR	CR	SIIR	SCR	SCR	SCR	SCR	SCR	BRT	BRT
La	<0.50	71.50	<0.50	2.40	1.70	7.40	3.30	0.50	<0.50	3.60	<0.50
Ce	0.60	<0.50	<0.50	<0.50	<0.50	0.70	<0.50	<0.50	<0.50	<0.50	<0.50
Pr	0.08	0.04	0.03	0.10	0.04	0.06	0.02	0.10	0.04	0.06	0.02
Nd	0.50	<0.40	<0.40	0.50	<0.40	<0.40	<0.40	<0.40	<0.40	<0.40	<0.40
Sm	0.10	<0.10	<0.10	0.30	<0.10	<0.10	<0.10	<0.10	<0.10	0.20	<0.10
Eu	0.07	<0.05	<0.05	0.15	<0.05	<0.05	<0.05	<0.05	<0.05	0.08	<0.05
Gd	0.36	0.20	0.12	0.54	0.07	0.08	0.06	0.06	<0.05	0.29	<0.05
Tb	0.07	0.05	0.04	0.12	0.01	0.01	<0.01	0.02	<0.01	0.05	0.01
Dy	0.36	0.33	0.17	0.79	<0.05	0.11	<0.05	0.10	<0.05	0.33	<0.05
Ho	0.10	0.09	<0.05	0.18	<0.05	<0.05	<0.05	<0.05	<0.05	0.08	<0.05
Er	0.25	0.29	0.13	0.43	<0.05	0.05	<0.05	0.09	<0.05	0.21	<0.05
Tm	<0.05	<0.05	<0.05	0.08	<0.05	<0.05	<0.05	<0.05	<0.05	<0.05	<0.05
Yb	0.25	0.24	0.10	0.45	<0.05	<0.05	<0.05	0.15	<0.05	0.20	<0.05
Lu	0.04	0.03	<0.01	0.05	<0.01	0.01	0.01	0.01	0.02	0.03	<0.01

Samples	MK 56-I	HMK 3	MK 98	MK 58	HMK 18	MK 122A	MK 162	MK 91	MK 89
Rock type	BRT	BRT	BRT	SER	SER	GR	GR	GR	GR
La	9.10	15.10	12.90	19.60	<0.50	1.50	5.10	25.50	2.50
Ce	32.10	25.50	19.80	<0.50	<0.50	2.50	12.90	48.70	5.40
Pr	2.34	3.33	2.72	0.03	0.04	0.31	2.05	5.61	0.75
Nd	10.00	15.80	10.80	<0.40	<0.40	2.30	10.80	21.20	3.40
Sm	2.20	3.30	2.20	<0.10	<0.10	0.70	3.80	4.30	1.30
Eu	0.60	0.90	0.65	<0.05	<0.05	0.29	0.97	1.00	0.31
Gd	2.45	2.92	1.92	<0.05	0.09	1.43	4.11	3.35	1.50
Tb	0.45	0.46	0.35	<0.01	<0.01	0.31	0.77	0.54	0.40
Dy	2.58	2.45	1.83	0.06	0.07	2.81	4.67	3.01	3.07
Ho	0.53	0.52	0.43	<0.05	<0.05	0.71	1.18	0.64	0.78
Er	1.38	1.39	1.28	<0.05	<0.05	2.26	3.19	1.77	2.56
Tm	0.19	0.25	0.22	<0.05	<0.05	0.35	0.57	0.31	0.42
Yb	1.13	1.36	1.39	<0.05	0.06	2.69	3.45	2.12	2.79
Lu	0.17	0.20	0.22	0.02	<0.01	0.39	0.56	0.25	0.43

(*Continues*)

DOI: 10.1002/gj

Table 3. (Continued)

Samples Rock type	MK 122A GR	MK 162 GR	MK 91 GR	MK 89 GR
Sc	6.00	11.00	13.00	15.00
Ba	29.00	24.00	267.00	41.00
Co	2.70	2.70	13.70	27.40
Hf	3.30	3.00	3.80	2.30
Nb	2.40	2.60	8.00	1.60
Rb	1.60	0.70	64.60	5.10
Sr	11.10	40.50	82.40	11.90
Ta	0.20	0.20	0.40	<0.10
Th	1.00	0.60	7.40	0.50
V	24.00	<5.00	117.00	75.00
Zr	110.30	90.50	141.50	70.80
Y	22.40	31.80	17.90	26.30
Cr	20.53	6.84	143.69	88.95
Mo	0.40	0.20	0.10	0.40
Cu	3.20	120.00	18.50	35.00
Pb	20.30	2.00	39.60	17.80
Zn	75.00	11.00	71.00	207.00
Ni	17.00	6.80	53.80	299.90
As	10.80	16.60	2.00	27.10
Sb	0.90	0.80	0.10	0.10
Ag	<0.10	<0.10	<0.10	<0.10
Au*	253.50	75.70	126.70	93.90
Hg	0.07	0.07	0.01	0.02
Tl	<0.10	<0.10	<0.10	<0.10

CR, carbonate rock; SIIR, silica- and iron-rich rock; SCR, silica-carbonate rock; BRT, birbirite; SER, serpentinite; GR, granitoid; n.a.; not analyzed.
*All of the trace elements except the Au are in ppm. Au values are in ppb.

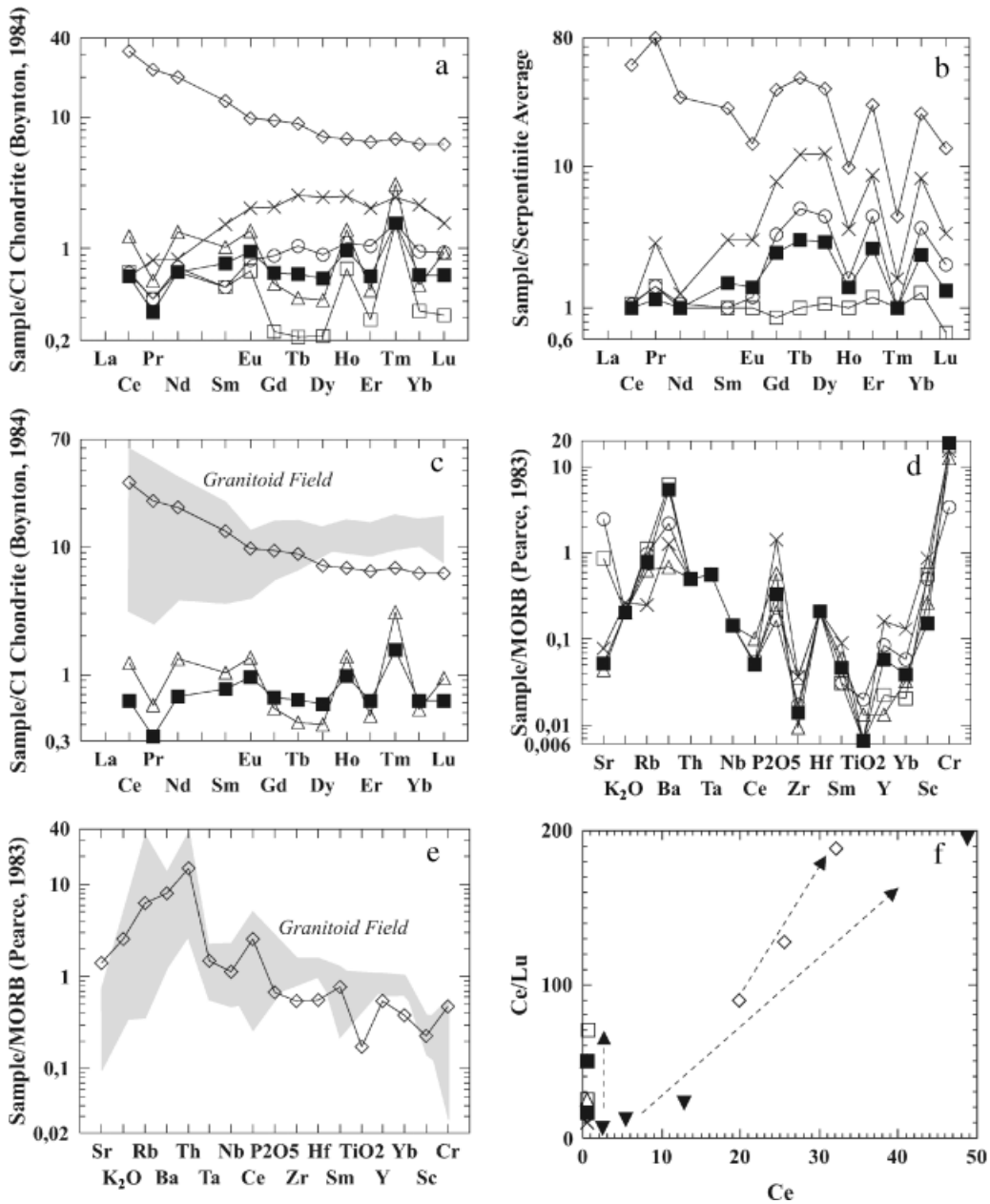

Figure 6. Chondrite normalized REE and MORB normalized spider diagram patterns of the host-rock serpentinite and the metasomatites. Normalization values are from Boynton (1984) and Pearce (1983) respectively. (△) serpentinite; (○) carbonate rocks; (□) silica-carbonate rocks; (■) group 1 birbirite; (◇) group 2 birbirite; (×) silica- and iron- rich sample (MK-26). Distribution of REE and trace element pattens of granitoid samples is shown by grey fields in **6c** and **6e**, and by (▼) in **6f**. (a) C1 chondrite normalized REE diagram of the metasomatites in the study area; (b) average serpentinite normalized REE diagram of the metasomatites; (c) C1 chondrite normalized REE diagram of granitoids, serpentinites, group 1 and group 2 birbirites; (d) MORB normalized trace element patterns of serpentinites, carbonate rocks, silica-carbonate rocks and group 1 birbirites; (e) MORB normalized trace element patterns of group 2 birbirites and granitoids; (f) fractionation in the trends of metasomatites on the Ce/Lu versus Ce binary plot.

DOI: 10.1002/gj

Group 2 birbirites suggest additional processes affecting the REE mobility in these rocks. C1 Chondrite normalized REE pattern distribution of the granitoid samples (Figure 6c – grey field) stack upon the pattern of Group 2 birbirites, whereas the trends of serpentinites and the Group 1 birbirites fractionate from the latter two. Figure 6c also shows that most of the granitoid samples are depleted in LREE, whereas the Group 2 birbirites are enriched in these elements.

Fractionation of REE patterns of the birbirite subtypes is also consistent with the trends on MORB normalized multi-element spider diagrams and the Ce/Lu versus Ce binary diagram (Figure 6f). On the spider diagrams, serpentinites, carbonate rocks, silica-carbonate rocks and Group 1 birbirites plot together and show high Cr contents (Figure 6d). In contrast, the patterns of Group 2 birbirites show lower Cr values and plot within the scatter range of the granitoid trend (Figure 6e). The same fractionation may also be observed in the Ce/Lu versus Ce diagram which indicate two exactly different trends for birbirite subtypes (Figure 6f).

Analyses of the base and precious metals indicate that the metasomatites of the Mihalıççık region are depleted in primary metal-sulphides of the serpentinites and enriched in elements which are abundant in low temperature environment. In general, most of the alteration products show a relative enrichment in Au, Ag, As, Ba, Sb and Sr, and depletion in Ni and Co according to the serpentinite (Figure 7a). The variation of Ni, As and Au in metasomatites and serpentinites of the study area is given on the Ni-As-Au ternary diagram in Figure 7b. Most of the samples plot along the Ni-As edge of the diagram due to low Au concentrations. Contrasting with depletion in Ni, introduction of As and Au is apparent with increasing silicification. A weak positive correlation between Ni and As values of the metasomatites becomes also significant with the progressive alteration (Figure 7c).

5. DISCUSSION

5.1. Genesis of the alteration

5.1.1. Thermodynamic conditions

Several authors suggested genetic models for formation of silica-carbonate assemblages (e.g. Auclair *et al.* 1993; Uçurum 1996, 2000), all of which include structural features (thrusts, faults or a micro-fractured and porous host-rock) as conduits for the hydrothermal fluid input. The thermodynamic conditions of the fluid are also generally discussed in several localities. For example, Auclair *et al*. (1993), in their paper on the Eastern Metals Ni-Cu-Zn deposits (Quebec Appalachians), suggested introduction of Ca, CO_2, S and As-rich solutions with low fO_2, fS_2 and high temperatures ($>350^\circ$) for carbonatization, and high fO_2 and fS_2 and moderate to low temperatures for silicification of the wall-rock. Uçurum (1996, 2000) suggested a fluid which evolves and changes in composition with water–rock interaction or two chemically different fluids that resulted in different alteration assemblages in the Divriği (Sivas) and Hekimhan (Malatya) districts, proposing lack of silica source, high pH (≥ 9), lower fO_2, lower formation temperatures or a combination of all these factors for the occurrence of carbonate assemblages.

The oxygen and sulphur fugacity (fO_2 and fS_2) are considered as dominant factors in formation of sulphide phases during serpentinization and following metasomatism (Groves *et al.* 1974; Eckstrand 1975; Groves and Keays 1979; Frost 1985; Auclair *et al.* 1993). Frost 1985 proposed that a CO_2-rich fluid infiltration within a primary peridotite at temperatures below 400°C can produce a significant amount of carbonate with a narrow margin of quartz and magnesite at the rims of the peridotite. He also noted that the oxygen fugacity will show a sharp rise in the carbonatized zone according to the extremely low fO_2 conditions at the serpentinization front and for a constant sulphur value in the rock, the fugacity of sulphur would vary sympathetically with that of oxygen. These arguments indicate that precipitation of sulphide species during the alteration require high fO_2 as well as high fS_2.

The pH and temperature of the fluid are also important factors that control the formation priority of the alteration assemblages. Changes in these conditions create temporal and/or spatial phase differentiations. Si solubility increases in high pH and high temperature environments, so the fluid input that caused the formation of silica must have had a lower pH and temperature during interaction with the wall-rock. On the contrary, absence of silica

DOI: 10.1002/gj

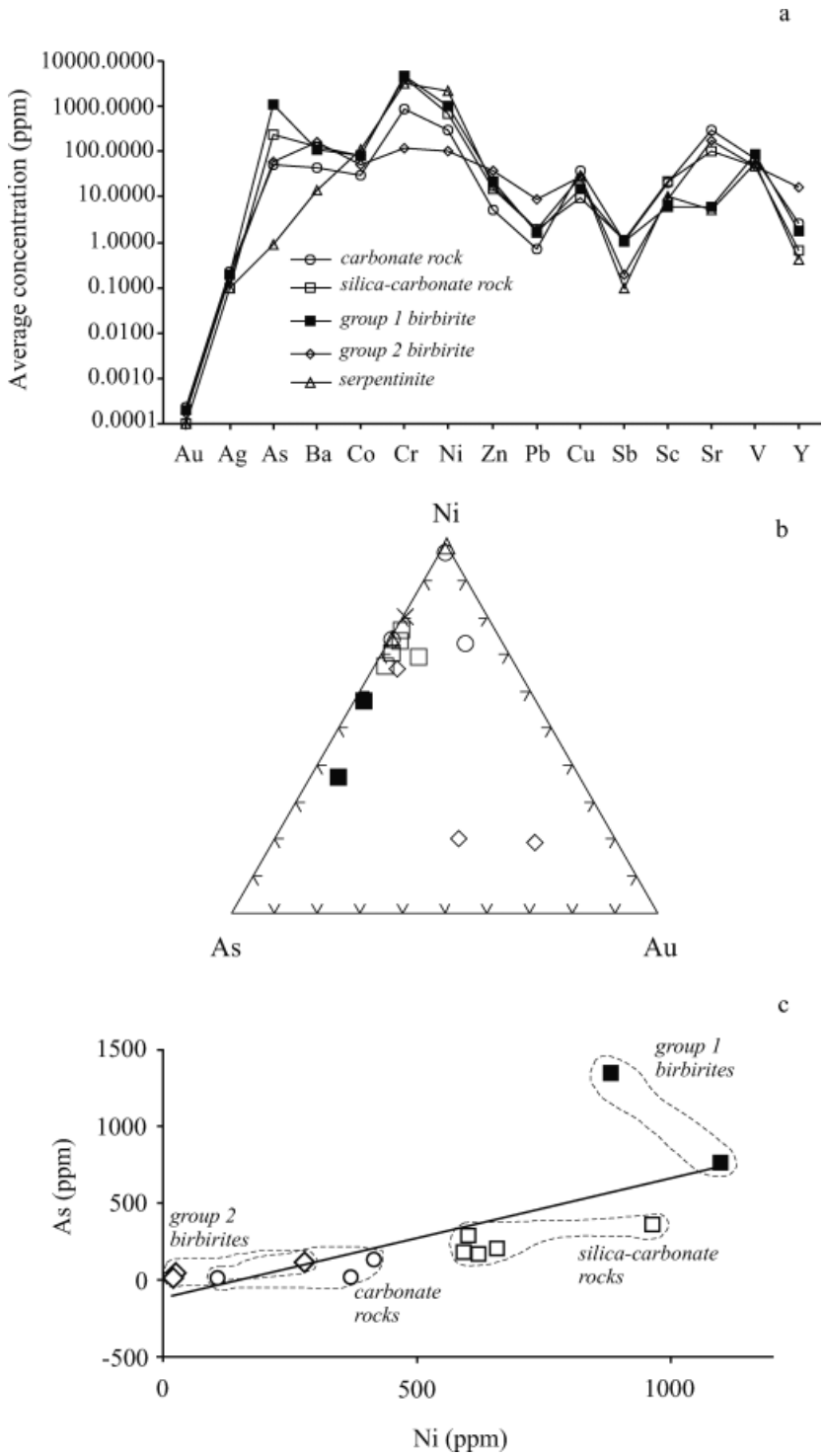

Figure 7. (**a**) Multiple element variation diagram of metasomatites and serpentinites in the study area; (**b**) Ni-As-Au ternary diagram of metasomatites and serpentinites in the study area; (**c**) Ni (ppm) versus As (ppm) binary diagram for the metasomatites. The symbol legend is as in Figure 6.

DOI: 10.1002/gj

indicates a higher pH and moderate to high temperature fluid (Uçurum, 2000), which holds the silica in solution and generates carbonate precipitation.

There are various studies on the formation temperature of the silica-carbonate assemblages. A maximum temperature range between 350 and 400°C is suggested for a stable quartz-dolomite assemblage at X_{CO_2} values varying between 0.1 and 0.5 at 1 kbar (Weir and Kerrick 1987; Auclair *et al.* 1993). Also, Spiridonov (1991) determined a formation temperature ranging between 340 and 280°C in CO_2-rich fluid inclusions in larger quartz grains of the listvenite-like metasomatites of the Zod gold deposit (Armenia). Craig (1973) proposed temperatures below 200°C for the presence of pyrite and millerite in listvenites and birbirites (Auclair *et al.* 1993). Thompson and Thompson (1996) defined the silica-carbonate alteration which is common in mercury and precious metal deposits of the epithermal type as a low-temperature, structure controlled event formed by CO_2-rich springs in a wide stability field ranging between 17 and 200°C. Rahmdohr (1969) indicated that marcasite is stable at temperatures up to 350°C; and this mineral can also be obtained by heating of cubanite to temperatures above 250°C. He also added that bravoite, the end-member of the FeS_2-NiS_2 mix-crystals series, occurs only at very low temperatures (up to 135°C). Referring to these notes and the paragenetic data of the alteration assemblages in the study area, we can suggest that the hydrothermal fluid continuously cooled during the alteration process.

5.1.2. Mode of occurrence

The formation of the alteration products in the study area can be explained by a multistage fluid influx model which is a combination of the models suggested by Auclair *et al*. (1993) and Uçurum (1996), 2000). In general, this genetic model is mostly consistent with the model given by Auclair *et al*. (1993), except the SiO_2 content of the percolating fluid. In the model suggested by the author, the infiltrating fluid is silica deficient and the SiO_2 component is gathered from the serpentine minerals. However, Figure 8a illustrates that the MgO content of the alteration rocks in the study area shows negative correlation with the increasing SiO_2 content during progressive alteration. Thus, to create sufficient silica saturation, additional silica must be introduced by the fluid in addition to the silica liberated from the serpentinites.

Mihalıççık metasomatite assemblages are primarily carbonatized during metasomatism. Thus, characteristics of the hydrothermal fluid are based on two basic assumptions in order to infer a model of genesis: (1) alkaline (high pH) nature; and (2) moderate to high temperature. The stages of metasomatism in the study area may be proposed as below with these assumptions (Figure 8b).

Tectonic activity creates fractures which will provide pathways for hydrothermal fluid input. A high temperature (above 350–400°C), high pH fluid bearing As, Ba, Sb, Sr and rich in SiO_2, Ca and CO_2, flushes through the fault or is strained upwards the fractures. Carbonatization of the rock takes place due to water–rock interaction and particularly dolomite ($(Ca,Mg)(CO_3)_2$) forms. Water is the source for Ca and CO_2, while rock is the source of Mg during metasomatism. A very small amount of As is added to the newly formed alteration assemblage due to high pH environment. Frost (1985) indicates that high fO_2 conditions in a H_2S-rich fluid should decrease the solubility of sulphides and result in precipitation of these phases. Sulphide assemblages are absent in the carbonate rocks in the study area. Hence, absence of even the primary sulphides of serpentinites in these dolomite-rich rocks may indicate dissolution of sulphides by a reducing, low fS_2 and H_2S-poor fluid at this very first stage of alteration.

At later stages, silica supersaturation takes place in the fluid due to the former carbonate precipitation and introduction of additional silica from the wall-rock (serpentinites). The input of previously dissolved sulphides into the fluid as H_2S species will decrease the pH of the slowly cooling fluid creating a weakly acid solution and resulting in silica precipitation. The decreasing temperature results in an increase in the Ca solubility. The depletion in Mg content in the environment due to previous dolomite crystallization and the limited Ca-solubility create small amounts of $CaCO_3$ in veins together with colloform silica. More As would leave the solution and join the silica precipitation as a result of decreasing pH forming the paragenesis of the silica-carbonate rocks. The sulphides which are dissolved during the carbonatization stage would reprecipitate in areas of higher fS_2 and fO_2 (Frost 1985). The occurrence of S-bearing low-temperature phases (e.g. marcasite) in the silica-carbonate rich rocks in the study area indicates increasing fS_2 and consequently fO_2 with decreasing temperature ($\leq$250°C) at the silicification stage. Schieber and Katsura (1986) proposed that the haematite precipitation in close proximity of

DOI: 10.1002/gj

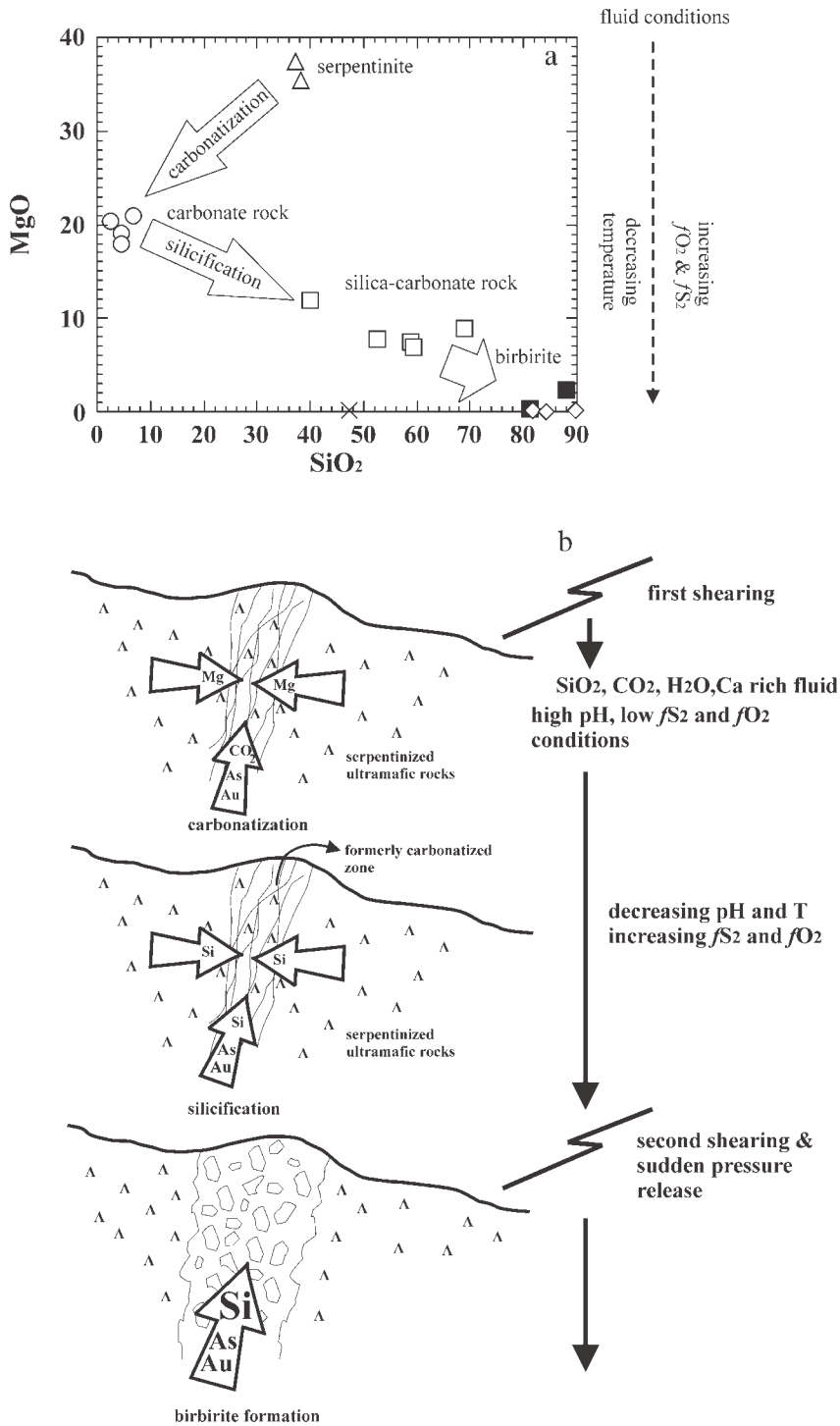

Figure 8. (**a**) MgO versus SiO_2 binary diagram showing the changes in the axis members during progressive alteration (The symbol legend is as in Figure 6); (**b**) the cartoon summarizing the metasomatism process.

DOI: 10.1002/gj

the sulphide minerals in Champion epithermal vein (Oregon-USA) is a result of either the sulphide deficient nature or the oxidizing state of the fluid. Similar to this case, the silica-rich and carbonate-free portions of the alteration assemblages in the study area are very rich in iron-oxides (Table 1), consistent with the increasing fO_2 during progressive alteration.

These proposed stages suggest a plausible timeline of events generating carbonate and silica-carbonate rocks, but the formation of the birbirites requires another stage. In the field, the birbirites are observed where the sharp turns in strike of the metasomatite outcrops are located. Hence, the location of the birbirites and mylonitization and ghosts of breccias in thin sections indicate that this intensive fine-crystalline silicification took place where the previous alteration assemblages are cross-cut by younger faults. Therefore, the tectonic activity must be the most effective factor on the last stage of alteration. The fractures in the study area may be filled with carbonates and quartz during the formation of carbonate and silica-carbonate rocks, obstructing the further fluid infiltration to the rock. Younger faults cross-cutting the pre-existing metasomatites, may create brecciation in these assemblages that results in opening of paths for new fluid infiltration. The sudden pressure release and the second fluid influx with this event would allow the pervasive amorphous silica precipitation. The arguments of Frost (1985), Schieber and Katsura (1986) and Auclair *et al*. (1993) note that the precipitation of arsenide-sulphide metallic phases with major amount of silica and accessory gold requires higher fS_2 and fO_2 at this last stage of alteration. The presence of bravoite in the birbirites suggests lower temperatures ($<135^{\circ}C$) for formation of these assemblages, which may be down to $17^{\circ}C$ as indicated by Thompson and Thompson (1996).

5.2. *Lack of mineralization*

Gold is transported via sulphide–arsenide complexes in the CO_2-H_2O-rich hydrothermal solutions (e.g. Buisson and Leblanc 1987; Leblanc and Fischer 1990) and precipitated during the introduction of silica (Buisson and Leblanc 1987). Buisson and Leblanc (1987) indicated that gold is associated with cobalt–arsenide mineralization in Bou Azzer (Morocco) ophiolite complex, whereas in the serpentinite massifs of the Arabian shield, it is associated with the pyrite-rich portions of gersdorffite (NiAsS)-bearing listvenite lenses and their 'en-échelon' late stage quartz veins. Leblanc and Fischer (1990), inferred that the ultramafic rocks are the source for Co and Au which are mobilized from the primary magmatic sulphide species during serpentinization. In addition, Auclair *et al*. (1993) noted that all of the alteration products in the Eastern Metals Ni-Cu-Zn Deposit are rich in Cr, Ni and Co. Consequently, the low temperature alteration assemblages in the ophiolitic terrains would show positive correlations between Ni, Au, As and Co.

Mihalıççık metasomatites do not include ore grade mineralization. Besides, these assemblages are depleted in Ni and Co relative to the host-rock, although there is a positive correlation between Ni and As in products of progressive alteration (Figure 7). This relation approves that the Ni-bearing phases of serpentinites are dissolved during carbonatization and reprecipitated as nickel–arsenide complexes due to the increasing sulphur and oxygen fugacity during silicification. However, the reprecipitation in silicification stage seems to provide insufficient amount of Ni to the newly formed assemblages. The only exception of this event is observed in the silica and iron-rich sample (*MK 26*) which show enrichment in Co and Ni and may indicate local peaks in the fO_2 and fS_2. Consequently, the lack of economic base-metal and precious metal sulphide mineralization in the study area may be related to the insufficient sulphur and oxygen fugacity of the hydrothermal solution as well as its sulphide deficient nature.

5.3. *Implications for strong REE patterns in Group 2 Birbirites*

The suggested thermodynamic conditions of the fluid influx enlighten the formation of carbonate rocks, silica-carbonate rocks and Group 1 birbirites in the study area. However, the enriched REE patterns of the Group 2 birbirites remain as a matter of debate. The spatial correlation of Group 2 birbirites with the granitoids and analogous REE patterns of both rocks suggest an interaction between these rocks during the last stage metasomatism. This consideration is also supported by approximately granitic Ni contents of the Group 2 birbirites.

DOI: 10.1002/gj

Most of the granitoid samples show LREE depletion, whereas the Group 2 birbirites reflect a significant LREE enrichment. McLennan (1989) indicated that water–rock interaction especially at low temperatures, is unlikely to cause substantial changes in REE distributions of most rocks. In contrast, weathering solutions with extreme chemistries (fO_2, pH and concentrations of complexing agents such as organic acids and chlorine ions) are favoured as potential transports for REE mobility (McLennan 1989). Thus, the effects of some kind of leaching and accumulation process may be considered for REE mobility in the Group 2 birbirites. Percolation of excessively CO_2 and organic-acid charged meteoric waters (Nesbitt 1979) may likely be agents to remove the LREE from the granitic lithologies into the solution. The REE are primarily recycled within the weathering profile rather than being transported significant distances in the solution (Nesbitt 1979; McLennan 1989). For this reason, Group 2 birbirites which are located near these washed (and leached) granitoid slices, can be affected from the REE migration. The products of this LREE enriched solution input into the system would be the Group 2 birbirites with enhanced REE patterns. As an alternative approach, the hydrothermal fluid movement during metasomatism may also be assumed as the trigger for similar leaching and accumulation processes for LREE in the metasomatites of the study area. Pirajno (1992) indicated that REE abundances would be significantly affected in a rock only if the hydrothermal fluid is flushed several times through the system. However, it must be noted that the temperature of the fluid must be much higher than the one during the formation of birbirites to provoke this kind of mobilization. In either approach, it may be suggested that the Group 2 birbirites are the last products of alteration.

6. CONCLUSIONS

Three types of metasomatites are determined in serpentinite host rocks of the Mihalıççık region; namely the carbonate rocks, silica-carbonate rocks and the birbirites. These assemblages comprise dolomite, quartz and dolomite, and very fine-crystalline quartz, respectively. Absence of fuchsite in the paragenesis indicates that these assemblages are not listvenites, but listvenite-like metasomatites.

The alteration assemblages of the Mihalıççık region are good examples for non-mineralized metasomatites of the listvenitic series. Their precious metal contents are elevated but not in ore grade. This result is consistent with the results of the General Directorate of Mineral Research and Exploration (MTA) of Turkey's Sivrihisar Polymetal Prospect.

Carbonatization and silicification and tectonics dominate the metasomatism processes in the Mihalıççık region (Eskişehir). The metasomatites of Mihalıççık indicate primary carbonatization and secondary silicification of the serpentinites. The carbonate rocks are the first products of alteration and are followed by silica-carbonate rocks. Formation of birbirites is related to reactivation of tectonic features. In this aspect, there is a similarity with the listvenites of the Kağızman region (Kars: Tüysüz and Erler 1993) and alteration assemblages of Eastern Metals Ni-Cu-Zn Deposits (Quebec: Auclair *et al*. 1993).

Au, Ag, Sb and Cu concentrations are relatively enriched in the alteration products, whereas As, Ba and Sr show significant enrichment. The limited precious and base metal enrichment indicates the lack of these metals in the CO_2-H_2O-SiO_2 rich solution.

The lack of sulphide assemblages in the carbonate rocks of the Mihalıççık region indicate that the primary sulphides of the serpentinites dissolved during carbonatization under low fS_2 and fO_2 conditions. The gradual increase in the sulphide assemblages and the Ni and Co values in the latter alteration products suggest that the dissolved sulphides are re-precipitated during silicification of the rock with increasing fS_2 and fO_2. However, in general, Ni and Co values of the alteration products are depleted according to the serpentinites suggesting inadequate elevation of these variables during the ore-forming processes.

The LREE enrichment in Group 2 birbirites and LREE depletion in the juxtaposed granitoid slices indicate that an interaction took place between these lithologies. This type of significant difference may occur due to the leaching of LREE's of the granitoids by meteoric fluid wash out. It may be speculated that the leaching process is of meteoric or of hydrothermal nature. However, to simulate this kind of leaching, the temperature of the fluid must be higher than the one during formation of the birbirites. Thus, the last suggestion is more unlikely.

DOI: 10.1002/gj

ACKNOWLEDGEMENTS

We are grateful to Sivrihisar Polymetal Prospect camp chief Necmettin Çeltek and the camp crew for their efforts on logistics, and to Dr Abidin Temel for performing XRD and XRF studies at Hacettepe University, Turkey. We are also indebted to Erdin Bozkurt, Yıldırım Dilek, Osman Parlak and Fatma Toksoy-Köksal for valuable critical comments on the earlier version of the paper.

REFERENCES

Abovian SB. 1978. Genetic types of listvenites of the Armenian Republic and their metallogenic significance. (Zapiski Armianskoe Otdelenie Vsesoiliznogo). *Mineralogichcskogo Obshchestva* **9**: 98–109.

Abu El-Enen MM, Okrusch M, Will TM. 2004. Contact metamorphism and metasomatism at a dolerite-limestone contact in the Gebel Yelleq area, northern Sinai, Egypt. *Mineralogy and Petrology* **81**: 135–164.

Akbulut M. 2003. Dümrek (Sivrihisar-Eskişehir) Yöresi Ofiyolitlerine Bağlı Cevherleşmelerin İncelenmesi [Investigation of Mineralizations Related to Dümrek (Sivrihisar-Eskişehir) Region Ophiolites]. MSc Thesis, Dokuz Eylül Üniversitesi, Turkey [unpublished, in Turkish with English abstract].

Ash CH, Arksey RL. 1990a. The listwanite-lode gold association in British Columbia. Geological Fieldwork 1989, a summary of field activities and current research, province of British Columbia. *Mineral Resources Division Geological Survey Branch*: 359–364.

Ash CH, Arksey RL. 1990b. *Tectonic Setting of Listwanite-related Gold Deposits in Northwestern British Columbia (104N/12)*. B. C. Ministry Energy, Mines and Petroleum Resources Open File 1990–22.

Auclair M, Gauthier M, Trottier J, Jébrak M, Chartrand F. 1993. Mineralogy, geochemistry, and paragenesis of the Eastern Metals serpentinite-associated Ni-Cu-Zn deposit, Quebec Appalachians. *Economic Geology* **88**: 123–138.

Aydal D. 1989. Gold-bearing listwaenites in the Araç Massif, Kastamonu, Turkey. *Terra Nova* **2**: 43–52.

Bailey EH, Everhart DL. 1964. Geology and Quicksilver Deposits of the New Almaden District, Santa Clara County, California. *U. S. Geological Survey Professional Paper* 360: 206.

Bok II. 1956. Listvenites, their special features, varieties and conditions of formation. (Listvenity, ikh osobennosti, raznovidnosti i usloviya obrazovaniya). *Izvestiya Akademii Nauk Kazakhskoi SSR. Seriya Geologicheskaya* **22**: 3–22.

Borodayevskiy NI, Borodayevskiy MB. 1947. *The Berezovsk Ore Field. (Berezovskoye rudnoye pole)*. Metallurgizdat: Moscow.

Botros NS. 2002. Metallogeny of gold in relation to the evolution of the Nubian Shield in Egypt. *Ore Geology Reviews* **19**: 137–164.

Boynton WV. 1984. Geochemistry of the rare earth elements: meteorite studies. In *Rare Earth Element Geochemistry*, Henderson P (ed.). Elsevier: Amsterdam; 63–114.

Boztuğ D, Larson LT, Yılmaz S, Uçurum A, Öztürk A. 1994. Alacahan yöresi (GD Sivas) lisfenitlerinin jeolojik konumu, mineralojisi ve değerli metal içeriği [Geological orientation, mineralogy and precious metal content of Alacahan district (SE Sivas) listvenites]. *Çukurova Üniversitesi Mühendislik-Mimarlık Fakültesi 15. Yıl Sempozyumu, Proceedings*, 123–138 [in Turkish with English abstract].

Buisson G, Leblanc M. 1985. Gold in carbonatized ultramafic rocks from ophiolite complexes. *Economic Geology* **80**: 2026–2029.

Buisson G, Leblanc M. 1986. Gold-bearing listwaenites (carbonatized ultramafic rocks) from ophiolite complexes. In *Metallogeny of Basic and Ultrabasic Rocks*, Gallagher JM, Ixer RA, Neary CR (eds). Transactions - Institution of Mining and Metallurgy: London; 121–132.

Buisson G, Leblanc M. 1987. Gold in mantle peridotites from Upper Proterozoic ophiolites in Arabia, Mali, and Morocco. *Economic Geology* **82**: 2091–2097.

Craig JR. 1973. Pyrite-pentlandite assemblages and other low temperature relations in the Fe-Ni-S system. *American Journal of Science* **273-A**: 496–510.

Delaloye M, Bingöl E. 2000. Granitoids from Western and Northwestern Anatolia: geochemistry and modelling of geodynamic evolution. *International Geology Reviews* **42**: 241–268.

Eckstrand RO. 1975. The Dumont serpentinite: a model for control of nickeliferous opaque mineral assemblages by alteration reactions in ultramafic rocks. *Economic Geology* **70**: 183–201.

Erler A, Larson LT. 1990. Genetic classification of gold occurrences of the Aegean region of Turkey. In *Proceedings of the International Earth Sciences Congress on the Aegean Regions*, 1990, Savaşçın MY, Eronat AH (eds). Dokuz Eylül University, IESCA Publications: **2**: 12–23.

Floyd PA, Yalınız MK, Göncüoğlu MC. 1998. Geochemistry and petrogenesis of intrusive and extrusive ophiolitic plagiogranites, Central Anatolian Crystalline Complex, Turkey. *Lithos* **42**: 225–241.

Frost BR. 1985. On the stability of sulfides, oxides, and native metals in serpentinite. *Journal of Petrology* **26**: 31–63.

Genç Y, Gorzawski H, Amstutz GC. 1990. Silica-carbonate-talc alteration of the serpentinite from Narman Karadağ Ophiolitic Complex (Erzurum-Turkey): Its mineral paragenesis and chemistry. In *Proceedings of the International Earth Sciences Congress on Aegean Regions*, 1990, Savaşçın MY, Eronat AH (eds). Dokuz Eylül University, IESCA Publications: **2**: 246–257.

Goncharenko AI. 1970. Auriferous listvenites as a new type of mineralization in the northern part of the Kuznetsk Alatau. Izvestiya Tomskogo Politekhnicheskogo Instituta (*Reports of the Tomsk Polytechnical Institute*) **239**: 110–114.

Goncharenko AI. 1984. Auriferous listwaenites as a new type of mineralization in the northern part of the Kuznetsk Alatau. *Reports of the Tomsk Polytechnical Institute (1970)(translated by Translation Bureau of Secretary State of Canada)* **239**: 110–114.

Göncüoğlu MC, Türeli K. 1993. Orta Anadolu ofiyoliti plajiyogranitlerinin petrolojisi ve jeodinamik yorumu (Aksaray-Türkiye) [Petrology and geodynamic interpretation of Central Anatolian ophiolite plagiogranites]. *Turkish Journal of Earth Sciences* **2**: 195–203 [in Turkish with English abstract].

DOI: 10.1002/gj

Göncüoğlu MC, Turhan N, Şentürk K, Özcan A, Uysal Ş, Yalınız MK. 2000. A geotraverse across northwestern Turkey: tectonic units of the Central Sakarya region and their tectonic evolution. In *Tectonics and Magmatism in Turkey and the Surrounding Area*, Bozkurt E, Winchester JA, Piper JDA (eds). Geological Society: London; Special Publications 173: 139–161.

Gorchakov PN, Lishnevskiy EN. 1982. Igneous activity and its relationship to tungsten mineralization in listvenite of the Tamvatney ore cluster, as inferred from geophysical data. *Doklady Akad. Nauk SSSR (1980)* **253**: 152–154.

Gözler MZ, Cevher F, Ergül E, Asutay HJ. 1997. *Orta Sakarya ve Güneyinin Jeolojisi [Geology of Central and Southern Sakarya Region].* Maden Tetkik ve Arama Genel Müdürlüğü Report No: 9973 [unpublished, in Turkish].

Grant JA. 1986. The isocon diagram-A simple solution to Gresens' equation for metasomatic alteration. *Economic Geology* **81**: 1976–1982.

Gresens RL. 1967. Composition-volume relationships of metasomatism. *Chemical Geology* **2**: 47–55.

Groves DI, Keays RR. 1979. Mobilization of ore-forming elements during alteration of dunites, Mt Keith, Betheno, Western Australia. *Canadian Mineralogist* **17**: 373–389.

Groves DI, Hudson DR, Hack TB. 1974. Modification of iron-nickel sulfides during serpentinization and talc-carbonate alteration at Black Swan, Western Australia. *Economic Geology* **69**: 1265–1281.

Halls C, Zhao R. 1995. Listvenite and related rocks: perspectives on terminology and mineralogy with reference to an occurrence at Cregganbaun, Co. Mayo, Republic of Ireland. *Mineralium Deposita* **30**: 303–313.

Harris NB, Kelley S, Okay Aİ. 1994. Post-collision magmatism and tectonics in northwest Anatolia. *Contributions to Mineralogy and Petrology* **117**: 241–252.

Ivan P, Jaros J, Kratochvil M, Reichwalder P, Rojkovic I, Spisiak J, Turanova L. 1985. *Ultramafic Rocks of the Western Carpathians, Czechoslovakia*. Geologicky Ustav Dionyza Stura [Geological Survey of Slovak Republic]: Bratislava; 258.

Kashkai MA, Allakhverdiev ShI. 1965. *Listvenites, Their Origin and Classification*. (Listvenity, ikh genezis i klassifikatsiia: Akad. Nauk Azerbaidzhanskoi SSR), Institut Geologii im. Akad. I. M. Gubkina; Izdat. Akad. Nauk Azerbaidzhanskoi SSR, Baku, 142 [in Russian].

Kashkai MA, Allakhverdiev ShI. 1971. New data on listvenite and rodingite metasomatites among ultrabasites. *Izvestiya Akademii Nauk SSSR Nauka*: 17–26.

Koç Ş, Kadıoğlu YK. 1996. Mineralogy, geochemistry and precious metal content of Karacakaya (Yunusemre-Eskişehir) listwaenites. *Ofioliti* **21**: 125–130.

Korobeynikov AF, Goncharenko AI. 1986. Gold in ophiolite complexes in the Altai-Sayan folded region. *Geokhimiya* **1**: 49–62.

Kuleshevich LV. 1984. Listvenites in the greenstone belts of Eastern Karelia. *Geologiya Rudnykh Mestorozhdenii (Geology of Ore Deposits)* **3**: 112–116.

Larson LT, Erler YA. 1992. Geologic setting and geochemical signature of twenty-two precious metal prospects in Turkey. In *1st International Symposium on Eastern Mediterranean Geology.* Geosound Special Issue: 9–28.

Leblanc M, Fischer W. 1990. Gold and platinum group elements in cobalt-arsenide ores: hydrothermal concentration from a serpentinite source-rock (Bou Azzer, Morocco). *Mineralogy and Petrology* **42**: 197–209.

Leblanc M, Lbouabi M. 1988. Native silver mineralization along a rodingite tectonic contact between serpentinite and quartz diorite (Bou Azzer, Morocco). *Economic Geology* **83**: 1379–1391.

Lisenbee AL. 1971. The Orhaneli ultramafic-gabbro thrust sheet and its surroundings: a progress report. In *Geology and History of Turkey*, 1971, Campbell AS (ed.). 349–368.

Lodochnikov VN. 1936. Serpentine and serpentinites of Ylchirsk and other related questions. Trudi CNLGRI, 38.

MacLean WH. 1990. Mass change calculations in altered rock series. *Mineralium Deposita* **25**: 44–49.

MacLean WH, Kranidiotis P. 1987. Immobile elements as monitors of mass transfer in hydrothermal alteration: phelps dodge massive sulphide deposit, Matagami, Quebec. *Economic Geology* **82**: 951–962.

Madu BE, Nesbitt BE, Muehlenbachs K. 1990. A mesothermal gold-stibnite-quartz vein occurrence in the Canadian Cordillera. *Economic Geology* **85**: 1260–1268.

McLennan SM. 1989. Rare earth elements in sedimentary rocks: Influence of provenance and sedimentary processes. In *Geochemistry and Mineralogy of Rare Earth Elements*, 1989, Lipin BR, McKay GA (eds). 169–196.

Murchison RI, de Verneuil E, von Keyserling A. 1845. *The Geology of Russia in Europe and the Ural Mountains*. **Volume I**, Geology, John Murray: London.

Nesbitt HW. 1979. Mobility and fractionation of rare earth elements during weathering of a granodiorite. *Nature* **279**: 206–210.

Nixon GT. 1990. *Geology and Precious Metal Potential of Mafic-Ultramafic Rocks in British Columbia: Current Progress*. Geological Fieldwork 1989, Paper 1990-1, a summary of field activities and current research, province of British Columbia. Mineral Resources Division Geological Survey Branch: 353–358.

Okay Aİ. 1984. Distribution and characteristics of the northwest Turkish blueschists. In *Geological Evolution of the Eastern Mediterranean*, Dixon JE, Robertson AHF (eds). Geological Society: London; Special Publications **17**; 455–466.

Okay Aİ. 1989. Tectonic units and sutures in the Pontides, northern Turkey. In *Tectonic Evolution of the Tethyan Region*, Şengör AMC (ed.). Kluwer: Dordrecht; 109–115.

Okay Aİ, Göncüoğlu MC. 2004. The Karakaya complex: a review of data and concepts. *Turkish Journal of Earth Sciences* **13**: 77–95.

Okay Aİ, Harris NBW, Kelley SP. 1998. Exhumation of blueschists along a Tethyan suture in northwest Turkey. *Tectonophysics* **285**: 275–299.

Okay Aİ, Kelley SP. 1994. Tectonic setting, petrology and geochronology of jadeite + glaucophane and chloritoid + glaucophane schists from northwestern Turkey. *Journal of Metamorphic Geology* **12**: 455–466.

Okay Aİ, Tansel İ, Tüysüz O. 2001. Obduction, subduction and collision as reflected in the Upper Cretaceous-Lower Eocene sedimentary record of western Turkey. *Geological Magazine* **138**: 117–142.

Pearce JA. 1983. Role of the sub-continental lithosphere in magma genesis at active continental margins. In *Continental Basalts and Mantle Xenoliths*, Hawkesworth CJ, Norry MJ (eds). Shiva: Nantwich; 230–249.

Pirajno F. 1992. *Hydrothermal Mineral Deposits, Principles and Fundamental Concepts for the Exploration Geologist*. Springer-Verlag: Berlin, Heidelberg, New York.

DOI: 10.1002/gj

Ploshko VV. 1963. Listvenization and carbonatization at thermal stage of Urushten Igneous Complex, North Caucasus. *International Geology Review* **7**: 446–463.

Rahmdohr P. 1969. *The Ore Minerals and Their Intergrowths*. Pergamon Press: Oxford, London, Edinburgh, New York, Toronto, Sydney, Paris, Braunschweig.

Reçber A, Koç Ş, Kadıoğlu YK. 1997. Geochemical and geostatistical determination of Yunusemre (Eskişehir) listwaenite. In *Symposium of 20th Anniversary of Education of Geological Engineering in Çukurova University, Abstracts*, 132.

Rollinson R. 1993. *Using Geochemical Data: Evaluation, Presentation, Interpretation*. Longman Scientific & Technical: Essex.

Rose G. 1837. *Mineralogisch-geognostiche Reise nach dem Ural, dem Altai und dem Kaspischen Meere. Volume 1: Reise nach dem nördlichen Ural und dem Altai*. C.W. Eichhoff (Verlag der Sanderschen Buchhandlung): Berlin.

Rose G. 1842. *Mineralogisch-geognostiche Reise nach dem Ural, dem Altai und dem Kaspischen Meere. Volume 2: Reise nach dem sudlichen Ural und dem Kaspischen Meere, Uebersicht der Mineralien und Gebirgsarten des Ural*. G.E. Reimer (Verlag der Sanderschen Buchhandlung): Berlin.

Schieber J, Katsura KT. 1986. Sedimentation in epithermal veins of the Bohemia mining district, Oregon, USA: interpretation and significance. *Mineralium Deposita* **21**: 322–328.

Şengör AMC, Yılmaz Y. 1981. Tethyan evolution of Turkey: a plate tectonic approach. *Tectonophysics* **75**: 181–241.

Şentürk K, Karaköse C. 1981. Orta Sakarya bölgesinde Liyas öncesi ofiyolitlerin ve mavi şistlerin oluşumu ve yerleşmesi [Formation and emplacement of Pre-liassic ophiolites and blueschists in Middle Sakarya Region]. *Türkiye Jeoloji Kurumu Bülteni* **24**: 1–10 [in Turkish with English abstract].

Shcherban IP. 1967. On the genesis of listvenites. *Doklady Akad, Nauk SSSR* **172**: 448–450.

Shcherban IP, Borovikova GA. 1969. Thermodynamic data on the genesis of listwanites and listwanitized rocks. *Doklady Akad, Nauk SSSR* **191**: 448–450.

Sherlock RL, Logan MAV. 1995. Silica-carbonate alteration of serpentinite: implications for the association of mercury and gold mineralization in northern California. *Exploration and Mining Geology* **4**: 395–409.

Sherlock S, Kelley SP, Inger S, Harris N, Okay Aİ. 1999. ^{40}Ar-^{39}Ar and Rb-Sr geochronology of high-pressure metamorphism and exhumation history of the Tavsanli Zone, NW Turkey. *Contributions to Mineralogy and Petrology* **137**: 46–58.

Spiridonov EM. 1991. Listvenites and zodites. *International Geology Review* **33**: 397–407.

Thompson AJB, Thompson JFH. 1996. *Atlas of Alteration: A Field and Petrographic Guide to Hydrothermal Alteration Minerals*. GAC Mineral Deposits Division: Canada.

Tomkeieff SI. 1983. *Dictionary of Petrology*. John-Wiley and Sons: New York.

Tüysüz N, Erler A. 1993. Geochemistry and evolution of listwaenites in the Kağızman region (Kars, NE-Turkey). *Chemie der Erde* **53**: 315–329.

Uçurum A. 1996. *Geology, Geochemistry and Mineralization of the Silica-Carbonate Alteration (Listwaenite) from Late Cretaceous Ophiolitic Melanges at Cürek-Divriği in Sivas Province and at Güvenç, Karakuz-Hekimhan in Malatya Province, Central East Turkey*. Ph. D. Thesis, University of Nevada Reno, USA [unpublished].

Uçurum A. 2000. Listwaenites in Turkey: perspectives on formation and precious metal concentration with reference to occurrences in East-Central Anatolia. *Ofioliti* **25**: 15–29.

Uçurum A, Larson LT. 1999. Geology, base-precious metal concentration and genesis of the silica-carbonate alteration (listwaenites) from late Cretaceous ophiolitic mélanges at Cürek-Divriği in Sivas province and at Güvenç, Karakuz-Hekimhan in Malatya province, central east Turkey. *Chemie der Erde Geochemistry* **59**: 77–104.

Weir RH, Kerrick M. 1987. Mineralogic, fluid inclusion, and stable isotope studies of several gold mines in the Mother Lode, Tuolumne and Mariposa Counties, California. *Economic Geology* **82**: 328–344.

Yalınız MK, Floyd PA, Göncüoğlu MC. 1996. Supra-subduction zone ophiolites of Central Anatolia: geochemical evidence from the Sarıkaraman Ophiolite, Aksaray, Turkey. *Mineralogical Magazine* **60**: 697–710.

DOI: 10.1002/gj